Biochimica et Biophysica Acta 1818 (2012) 1663–1672

Contents lists available at SciVerse ScienceDirect

Biochimica et Biophysica Acta

journal homepage: www.elsevier.com/locate/bbamem

Binding of cationic pentapeptides with modified side chain lengths to negatively charged lipid membranes: Complex interplay of electrostatic and hydrophobic interactions

Maria Hoernke [1], Christian Schwieger, Andreas Kerth, Alfred Blume *

Institute of Chemistry, Martin-Luther-University Halle-Wittenberg, von-Danckelmann-Platz 4, D-06120 Halle (Saale), Germany

ARTICLE INFO

Article history:
Received 19 August 2011
Received in revised form 19 February 2012
Accepted 5 March 2012
Available online 11 March 2012

Keywords:
Pentapeptide
Peptide binding
DPPG
Hydrophobic interaction
Electrostatic interaction

ABSTRACT

Basic amino acids play a key role in the binding of membrane associated proteins to negatively charged membranes. However, side chains of basic amino acids like lysine do not only provide a positive charge, but also a flexible hydrocarbon spacer that enables hydrophobic interactions. We studied the influence of hydrophobic contributions to the binding by varying the side chain length of pentapeptides with ammonium groups starting with lysine to lysine analogs with shorter side chains, namely ornithine (Orn), α,γ-diaminobutyric acid (Dab) and α, β-diaminopropionic acid (Dap). The binding to negatively charged phosphatidylglycerol (PG) membranes was investigated by calorimetry, FT-infrared spectroscopy (FT-IR) and monolayer techniques. The binding was influenced by counteracting and sometimes compensating contributions. The influence of the bound peptides on the lipid phase behavior depends on the length of the peptide side chains. Isothermal titration calorimetry (ITC) experiments showed exothermic and endothermic effects compensating to a different extent as a function of side chain length. The increase in lipid phase transition temperature was more significant for peptides with shorter side chains. FTIR-spectroscopy revealed changes in hydration of the lipid bilayer interface after peptide binding. Using monolayer techniques, the contributions of electrostatic and hydrophobic effects could clearly be observed. Peptides with short side chains induced a pronounced decrease in surface pressure of PG monolayers whereas peptides with additional hydrophobic interactions decreased the surface pressure much less or even lead to an increase, indicating insertion of the hydrophobic part of the side chain into the lipid monolayer.

1. Introduction

The function of membrane associated proteins usually depends on their binding to biological membranes. So-called membrane binding tags play a key role in membrane association of proteins. These tags are often located at one end of the protein and contain positively charged amino acid residues like arginine, histidine, or lysine [1–5]. Antimicrobial peptides are important components for the defense of animals or plants against invading pathogenic microorganisms [6–9]. They are typically relatively short peptides with several positively charged amino acids and act by permeabilizing the target membrane. Their selectivity is based on the electrostatic attraction to negatively charged bacterial membranes, leaving the zwitterionic outer leaflet of eukaryotic membranes mostly unaffected. Their interactions are supposed to be mainly electrostatic in nature, especially at low peptide concentrations [10–14].

In contrast to naturally occurring peptide sequences, [15] simplified model peptides are especially useful for systematic investigations of the relation between structure and binding properties. Besides homopeptides (Lys_7 [13], Lys_{1-5} and Arg_{1-5} [3]), also sequences including hydrophobic and charged residues are of interest [16–18]. Besides providing a positive charge necessary for electrostatic interactions, side chains of basic amino acids like lysine also provide a hydrocarbon spacer which can mediate hydrophobic interactions with the membrane. The interplay of the electrostatic and hydrophobic interactions has rarely been considered so far. As a useful model system, polylysines (PLL) were widely studied with regard to electrostatic binding to negatively charged membranes. An increase in the lipid main phase transition temperature T_m after binding was observed in several studies [19–22]. In a more detailed study, long PLLs increased T_m while short PLLs decreased T_m. Furthermore, a

Abbreviations: Lys, lysine; Orn, ornithine; Dab, α, γ-diaminobutyric acid; Dap, α, β-diaminopropionic acid; FT-IR, Fourier-transform infrared; ITC, isothermal titration calorimetry; DSC, differential scanning calorimetry; PG, phosphatidyl glycerol; DPPG, 1,2-palmitoyl-*sn*-glycero-3-phosphoglycerol; DMPG, 1,2-myristoyl-*sn*-glycero-3-phosphoglycerol; POPG, 1-palmitoyl-2-oleoyl-*sn*-glycero-3-phosphoglycerol; TFA, Trifluoroacetic acid; Arg, arginine; PLL, poly-L lysine; MARCKS, myristoylated alanine-rich C-kinase substrate

* Corresponding author. Tel.: +49 345 5525850; fax: +49 345 5527157.
E-mail address: alfred.blume@chemie.uni-halle.de (A. Blume).
[1] Current address: Interfaces Department, Max-Planck-Institute of Colloids and Interfaces, Research Campus Golm, D-14424 Potsdam, Germany.

0005-2736/$ – see front matter © 2012 Elsevier B.V. All rights reserved.
doi:10.1016/j.bbamem.2012.03.001

stronger lipid interchain vibrational coupling and less disorder in the whole temperature range was found [23]. X-ray investigations revealed an unaltered chain packing within the bilayers after binding of PLL [24]. Short lysine peptides (up to 7 residues) interact with negatively charged lipids, but do not significantly interact with zwitterionic ones [3]. Pentalysine is a simple model for the MARCKS effector region protein, being identical with its first five residues [4,25]. The α-amino group at the end of the peptide does not contribute significantly to the binding [3]. In systems containing PS, PC and $(Lys)_6Trp$, bridging of adjacent bilayers was observed [26]. High peptide concentrations can even reverse the charge of the vesicles [3,13]. Mosior et al. [18] investigated pentalysine binding to PC/PG mixtures and found reduced affinity when Ala was alternately included in between the Lys residues, decreasing the charge density while keeping the number of five Lys residues constant. Compared to arginine peptides, lysine peptides are less easily internalized into cells [27]. It was reported that lysine residues did not penetrate into the lipid head group region [11,28,29]. Purely electrostatic binding and a small contribution of entropy to the adsorption free energy was deduced from theoretical estimates of binding thermodynamics [30]. As examined by spin-label electron spin resonance, [31] pentalysine has more influence on lipid chain mobility for negatively charged than for zwitterionic lipids. The lipid main phase transition temperature T_m of DMPG was broadened and decreased by −1 K, which could indicate that other than electrostatic influences are operative. There is a controversy about the formation of domains enriched in acidic lipids upon pentalysine binding [13,32].

Already de Kroon et al. [33] considered the role of charge and hydrophobicity. They investigated a series of short model peptides and concluded, that besides general electrostatic effects the position of charges on the peptide surface and hydrophobic interactions play a role. Because of unclear and controversial findings, we focus here on the effects of the hydrophobic spacer length on the binding to discriminate electrostatic and possibly concealed hydrophobic contributions.

To gain deeper insight into the role and magnitude of the contributions from hydrophobic interaction to the binding of positively charged oligopeptides, we used a set of tailor-made model peptides of amino acid analogs to lysine with reduced side chain length. These are pentaornithine (Orn_5); penta α, γ-diaminobutyric acid (Dab_5) and penta α, β-diaminopropionic acid (Dap_5) having three to one CH_2-groups in the side chain (Fig. 1). The short pentapeptides used in this study are not able to adopt defined secondary structures and therefore enable the study of electrostatic and hydrophobic contributions exclusively. The thermodynamics of the peptide binding to the lipids as well as the properties of the complex formed were determined by microcalorimetry (isothermal titration calorimetry (ITC) and differential scanning calorimetry (DSC)). Temperature-dependent Fourier-transform infrared spectroscopy (FTIR) of mixtures containing DPPG vesicles and peptides revealed changes in lipid organization and hydration. Injection of peptides underneath lipid monolayers spread on a Langmuir trough with fixed surface area assessed the adsorption of the peptides at different lipid packing conditions. We will show that the influence of the peptides on the lipid phase behavior and organization depends on the side chain length of the peptide so that the individual contributions of electrostatic and hydrophobic interactions can be distinguished.

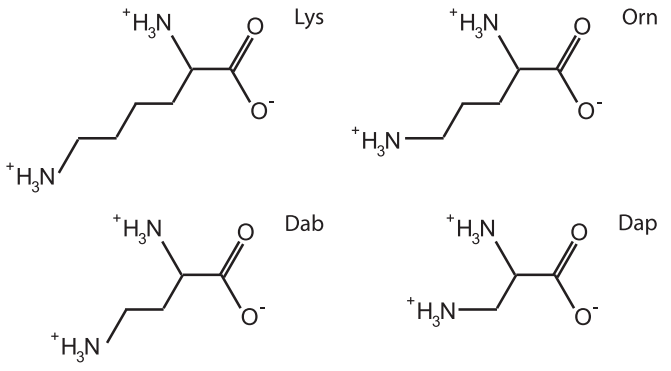

Fig. 1. Chemical structures of amino acids used for homopentapeptides: lysine (Lys), ornithine (Orn), α, γ diaminobutyric acid (Dab) and α, β diaminopropionic acid (Dap).

2. Materials and methods

2.1. Materials

Pentapeptides were custom-synthesized in the Leibniz-Center for Medicine and Biosciences, Borstel, Germany. The TFA counter ion was exchanged by adding 0.5 M HCl and lyophilizing the solution three times [34]. The lipids 1,2-myristoyl-*sn*-glycero-3-phosphoglycerol (DMPG) and 1,2-palmitoyl-*sn*-glycero-3-phosphoglycerol (DPPG) were purchased from Lipoid GmbH, Ludwigshafen, Germany, and used without further purification. Solvents and organic compounds were purchased from Carl Roth GmbH, Karlsruhe and used without further purification. D_2O and DCl were purchased from Sigma-Aldrich, St. Louis, USA. For all other experiments ultra-pure water with a conductivity of less than 0.55 μS cm^{-1} was used.

2.2. Sample preparation

For DSC and ITC experiments, lipids were dispersed in aqueous solution containing 100 mM NaCl by heating the sample above the phase transition temperature and intense vortexing. Vesicles were sized by extrusion through a 100 nm polycarbonate membrane using a Liposo-Fast-Extruder (Avestin). The vesicle size was determined by dynamic light scattering using an ALV-NIBS/HPPS particle sizer (ALV-Laser Vertriebsgesellschaft mbH., Langen, Germany). Phosphorous analysis as described in Ref. [35] was used to determine the lipid concentration. For ITC ~20 mM solutions were used whereas for DSC the suspensions had a concentration of ~2 mM. For IR spectroscopic measurements lipids were dispersed in 100 mM NaCl solution and sonicated at temperatures above phase transition temperatures for 2 h in a water bath to yield solutions with a lipid concentration of 60 mM. For film balance experiments lipid stock solutions in chloroform with a small amount of methanol and a concentration of 0.7 mM were prepared. The concentration of the peptide solutions was adjusted according to the desired lipid head group to peptide charge ratio $R_c = 1$, i.e. 60 mM peptide monomeric units for FTIR and 2 mM peptide monomeric units for calorimetric experiments. The stock solution used for injection into a subphase of the film balance trough was 15 mM peptide monomeric units. The injection volume was adjusted to obtain a concentration of 15 μM based on peptide monomer units.

2.3. Isothermal titration calorimetry

ITC was performed using a MicroCal VP-ITC (MicroCal Inc., Northampton, USA). Suspensions of vesicles (20 mM) were injected into the peptide (2 mM based on the monomeric units) solutions in steps of 10 μL at temperatures of 25 °C and 50 °C. Time between two injections was 600 s or 900 s. Data were baseline corrected, integrated and normalized to the concentration of the lipid using the ORIGIN software.

2.4. Differential scanning calorimetry

DSC was performed with a MicroCal VP-DSC (MicroCal Inc., Northampton, USA). Before the calorimetric experiments, the solutions were degassed and then filled into the sample cell. In all experiments we used a heating rate of 1 °C min^{-1} and a time resolution of

4 s. Lipid and peptide samples were prepared separately and mixed directly before measurement. The concentration based on peptide monomeric units and the lipid concentration in the calorimetric cell were always 1 mM. As a reference a 100 mM NaCl solution was used. At least three up and down scans were performed for each sample to prove the reproducibility. All curves shown in the figures originate from the third heating scan. Integration using the ORIGIN software yielded the lipid main phase transition enthalpy ΔH_m.

2.5. FTIR spectroscopy

FT-IR-spectra were recorded using Bruker Vector 22 spectrometer (Bruker GmbH, Germany) equipped with a DTGS detector. Lipid and peptide samples were prepared separately and mixed directly on the CaF_2 window before measurement. The samples containing lipids (60 mM) and pentapeptides (60 mM based on peptide monomeric units) in D_2O were placed between two CaF_2 windows, which were separated by a Teflon spacer of 56 μm thickness. The hollow sample mount was thermostated by an external circulating water bath (Haake F3C, Gebr. Haake GmbH, Karlsruhe, Germany). Temperature was incremented in steps of 2 K and equilibrated for 8 min after each step. 32 scans with a spectral resolution of 2 cm^{-1} were collected and Fourier transformed after one level of zero filling. For data processing, the Bruker OPUS FT-IR software was used. Spectra of a 100 mM NaCl solution in D_2O were used as reference and subtracted from the sample spectra [36]. Peak positions were determined by the second derivative method. Carbonyl and amide bands were decomposed using Gaussian–Lorentzian functions (80% Gaussian). Intensities and full width at half maximum values for amide bands were taken from pure peptide measurements and kept constant for decomposition in spectra taken from lipid–peptide mixtures.

2.6. Monolayer experiments

Monolayer experiments were carried out in a home-made circular trough equipped with a HAAKE thermostating system and kept at 20 °C for all experiments. The fixed area of the trough was 7.068 cm^2, its volume was 10.2 mL. 100 mM NaCl solution was filled into the trough for all experiments. Surface tension was recorded using the WILHELMY plate sensor (Riegler and Kirstein, Potsdam, Germany). The subphase was stirred with a small magnetic stirring bar during all experiments. A certain volume of the lipid stock solution was spread onto the surface to give the desired starting pressure. After equilibration of the system, 10 μL of peptide stock solution (15 mM based on monomeric units) were injected through a laterally drilled hole into the subphase yielding a concentration of 15 μM peptide monomeric units. The surface tension was recorded for at least 2 h after injection. The whole system was covered by a Plexiglas hood to prevent contamination during the measurements.

3. Results and discussion

3.1. Binding studies

3.1.1. Isothermal titration calorimetry

Binding constants, binding enthalpies, and stoichiometry of the lipid–peptide complexes were determined by ITC measurements. In Fig. 2, the heat flow (upper panel) and integrated heats of binding (lower panel) of DPPG vesicles to Dab_5 (monomers as in Fig. 1) are shown as an example. DPPG was chosen, because it allows to study binding to the gel state as well as to the liquid–crystalline phase in a temperature range that is experimentally easily accessible. With T_m(DPPG) = 41 °C, measurements below (25 °C) and above (50 °C) the lipid main phase transition temperature were carried out. DPPG vesicles were titrated into the peptide solution and the heat flow was recorded. The heat flow of the titration of gel state vesicles

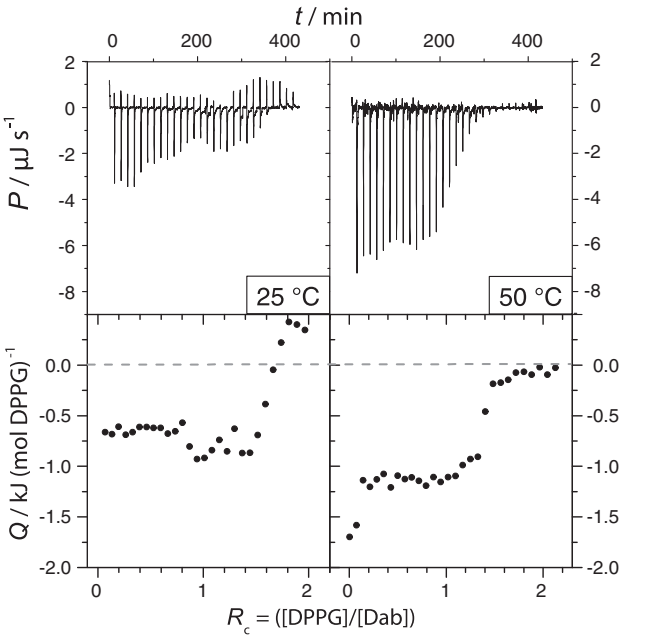

Fig. 2. ITC data of the titration of extruded DPPG vesicles (d = 100 nm) into a Dab_5 solution at 25 °C and 50 °C from left to right. Upper panels: heat flow, baseline corrected, lower panels: integrated heats of titration with respect to the charge ratio R_c = ([DPPG]/[Dab monomeric unit]) (100 mM NaCl, 2 mM Dab_5 monomeric units in the cell, 20 mM DPPG in the syringe).

into Dab_5 (upper panels of Fig. 2), shows two distinctly different processes. Each injection leads to a fast endothermic followed by a slower exothermic heat response. The lower panels of Fig. 2 show the integrated heats of injection, where these individual effects are not resolved. Due to the decreasing amount of free peptide in the cell, the injection enthalpies decrease with each consecutive injection. The last injections correspond to the dilution heat of the vesicles. Assuming that the binding constant is sufficiently high, the sum of all reaction heats gives the total binding enthalpy $\Delta_b H$ from which the molar binding enthalpy can be calculated, knowing the total amount of peptide in the cell.

We studied the interaction of DPPG with the pentapeptides in the order of decreasing side chain lengths (monomers as in Fig. 1). The results are summarized in Fig. 3A. Binding of Lys_5 to DPPG vesicles was endothermic at all temperatures at the beginning of the titration, hence at low lipid:peptide monomer ratios R_c. The total heat per injection step changed from endothermic to exothermic at a certain ratio R_c (>0.8 and >1.4 for 25 °C and 50 °C, respectively), even though exothermic as well as endothermic contributions are still visible in the titration peaks (not shown). Titration of fluid phase vesicles was more endothermic than titration of gel phase vesicles to the peptide solution.

Similar behavior was observed titrating DPPG vesicles into Orn_5 solutions. Comparable to the binding of Lys_5, the change in overall interaction heats from endothermic to exothermic occurs at lower R_c-values (>0.2 and >1.3 for 25 °C and 50°, respectively). Again, the heat of reaction with the lipids was more endothermic for fluid phase vesicles compared to gel phase vesicles.

A further decrease in the length of peptide side chains without altering the number of charges leads to Dab_5. Titration of DPPG vesicles into Dab_5 solutions showed almost only exothermic heats at all R_c-values and temperatures (see also example in Fig. 2). The heat per titration step becomes more negative until endothermic contributions nearly vanished (R_c = 1.7 at 25 °C). At 50 °C, a sigmoidal decrease in exothermic heat was observed. In contrast to the peptides with longer side chains, titration of fluid phase vesicles to Dab_5

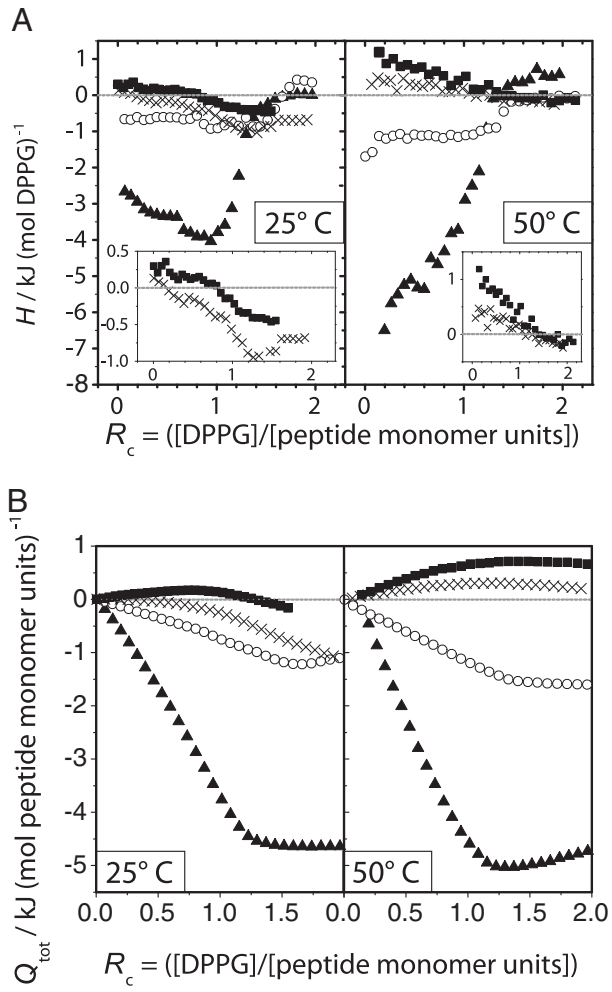

Fig. 3. Enthalpies determined from ITC titration of DPPG vesicles ($d = 100$ nm) into peptide solutions: Lys_5 (filled squares), Orn_5 (crosses), Dab_5 (open circles), and Dap_5 (filled triangles) at 25 °C in the gel phase of the vesicles and at 50 °C in the fluid phase of the vesicles (100 mM NaCl, 2 mM pentapeptide monomeric units in the cell, 20 mM DPPG in the syringe injected in steps of 10 μL with 600–900 s waiting time). A: integrated heats per titration step normalized to the added lipid concentration. The insets are enlarged data of Lys_5 and Orn_5 titrations. B: Total heat of reaction Q_{tot}^{cell} per mol of peptide monomer unit in the cell.

yielded more exothermic binding enthalpies than titration of gel phase vesicles.

For Dap_5, the peptide with the shortest side chains, similar curves showing a sigmoidal decay of the exothermic heat of binding were recorded. At $R_c = 1.6$, only minimal heats of dilution were detected. The released heat was larger after injection of fluid phase vesicles than of gel phase vesicles, similar to the Dab_5 system.

In general, it can be concluded that at least two superimposed processes take place. For the interaction of DPPG with Lys_5 the overall binding was endothermic. For peptides with shorter amino acid side chains the binding enthalpy gradually decreased and became more exothermic, so that the interaction with Dab_5 and Dap_5 was finally completely exothermic. For Dap_5, the detected heats per injection were significantly more exothermic than expected from the tendency observed with the other peptides. The *pK* value of the Dap_5 side chain is expected to be lower than the *pK*-values for the side chains of the other peptides [37], because of the possibility of an intramolecular H-bond between the Dap side chain amide group and the carbonyl group in the peptide bond. However, at the highly charged lipid bilayer surface, a change in the apparent *pK* is expected, since the creation of the positive charge leads to a gain in free energy in the presence of a negative surface potential. The intrinsic pK_0 observed for molecules in solution and the apparent pK_{app} observed at a bilayer surface having a surface potential ψ_0 are related by $pK_{app} = pK_0 - ze\psi_0/(2.303kT)$ [38]. For a surface potential of ca. −132 mV for a PG bilayer in 100 mM salt (calculated from the Gouy–Chapman theory) (see Träuble et al. [39] and Tocanne [38]) one would calculate a shift of the pK_{app} of 2.18 units to higher values, i.e. from ca. 6.33 to 8.51. This would then lead to a fully charged Dap_5 peptide. This means that upon Dap_5 binding protonation occurs and the heat of protonation is detected as an exothermic contribution to the total binding enthalpy.

For peptides with short side chains (Dab_5 and Dap_5), binding enthalpies of vesicles in the fluid state were clearly more exothermic than that of gel state vesicles. Peptides with longer side chains (Lys_5 and Orn_5) showed the opposite effect. Here the binding to gel phase vesicles was more exothermic than to fluid phase vesicles.

The interaction of Dab_5 with negatively charged lipids is expected to be predominantly electrostatic, as the peptide does not provide enough hydrophobic surface for hydrophobic interactions. The binding of Dab_5 to DPPG vesicles was exothermic. Therefore, we assume electrostatic binding to be purely exothermic in the chosen model system. With increased hydrocarbon side chain length, hydrophobic interactions are more likely to occur. We find a gradually less exothermic binding enthalpy for Orn_5 and Lys_5 that could be the sum of the constant exothermic binding due to electrostatic interactions and the increased endothermic contribution due to hydrophobic interactions. In particular, we observed an overcompensation of the exothermic effect by an endothermic effect when Lys_5 was bound to DPPG vesicles.

Endothermic processes are entropy driven. They can occur due to a dehydration of the peptide, if water is released from hydration shells during the interaction [40–42]. Also, dehydration of lipid head groups due to insertion of peptide side chains would be such an entropically drive process.

3.1.2. Binding enthalpy $\Delta_b H$ and binding constant K

No standard binding model could be used to fit the titration data of Lys_5 and Orn_5 binding due to the continuously changing reaction heat at low R_c-values. Therefore, *K* and $\Delta_b H$ values could not be obtained. However, the small endothermic binding enthalpy for Lys_5 binding agrees with previous observations. Montich et al. reported that the titration of Lys_5 to POPG yielded small and positive binding enthalpies that depended on vesicle size [43]. $\Delta_b H$ for Lys_5 binding to small sonicated POPG vesicles was 4.2 kJ mol^{-1} and binding to large unilamellar vesicles yielded a binding enthalpy of 0 kJ mol^{-1} [43].

The titration of DPPG vesicles into Dab_5 and Dap_5 solutions resulted in binding heats that showed a sigmoidal decrease of the titration curve. A model with one set of sites could be used to fit the data. $\Delta_b H$ is −1 to −6 kJ mol^{-1} and K is in the order of 10^5 M^{-1} (Table 1). The binding constants of Dab_5 and Dap_5 to DPPG decreased slightly with increasing temperature. Binding of Dap_5 to DPPG seems to be slightly weaker than for the longer side chain peptide Dab_5.

To be able to gain information on the data that could not be fitted, the following equation was used to calculate the accumulated

Table 1
Binding enthalpies $\Delta_b H$ and binding constants *K* for the binding of DPPG to Dab_5 and Dap_5 obtained by ITC: fitting of a One-Set-of-Sites-Model to the data. All given values are normalized to 1 mol peptide monomeric units (100 mM NaCl, 2 mM pentapeptides based on monomeric units in the cell, 20 mM DPPG in the syringe).

Sample	$\Delta_b H$/kJ mol^{-1}		$K/10^5$ M^{-1}	
	25 °C	50 °C	25 °C	50 °C
DPPG + Dab_5	−0.7	−1.1	5.4	1.8
DPPG + Dap_5	−3.4	−5.8	2.8	0.3

total heat of reaction per mol of peptide monomer units in the cell content:

$$Q_{\mathrm{tot}}^{\mathrm{cell}} = \sum_i \frac{Q_{\mathrm{i}}^{\mathrm{inj}}\left(1+\left(\frac{\sum_{\mathrm{i}} V_{\mathrm{i}}^{\mathrm{inj}}}{V_{\mathrm{cell}}}\right)\right)}{c_{\mathrm{cell}}^{0} V_{\mathrm{cell}}}$$

with i being the injection number, $Q_{\mathrm{i}}^{\mathrm{inj}}$ and $V_{\mathrm{i}}^{\mathrm{inj}}$ the heat and the volume of injection, V_{cell} the cell volume and c_{cell} the concentration of the reactant (peptide monomeric units) in the cell before the first injection. Fig. 3B shows that the total heats of reaction are exothermic for short side chain peptides and lipids in the gel phase and even more exothermic for lipids in the fluid phase. For long side chain peptides, the total heat of reaction is close to zero or slightly endothermic. Comparison of the binding of the long side chain peptides to gel state and fluid vesicles shows that binding to fluid state vesicles is more endothermic than to gel state vesicles.

3.1.3. Stoichiometry of binding

The stoichiometry of binding was determined from the saturation concentration when Q_{tot} stayed almost constant after further injections. This yields a value of about 1.5 DPPG molecules per peptide monomeric unit. This might be due to one or more effects including overcharging, [44] permeability of the vesicles [45] or precipitation. Although we consider permeability of the vesicles as the most probable reason, ultimately it cannot be decided which processes take place, since these have contrary effects and may also compensate.

3.2. DSC studies of the lipid–peptide complexes

Differential scanning calorimetry measurements (DSC) were performed to reveal the influence of peptide binding on the lipid phase transition. Fig. 4 shows the influence of peptide binding on the transition behavior. In the mixed DPPG–peptide samples with complete charge compensation ($R_c = 1$), the pretransition is completely suppressed. Compared to pure DPPG, broad peaks and several maxima indicate that the phase transitions of lipid–peptide mixtures are complex processes. The melting temperature (T_{melt}) was determined from the most prominent maximum of the C_p-curve in the heating scans and the values are shown in Table 2 together with T_{mid}, obtained from the midpoint of the integral of the curves. In all lipid–peptide complexes T_{melt} increased after peptide binding. The most pronounced effect was observed after binding of Dap_5, the peptide with the shortest side chains. For the peptides with longer side chains, we found that the increase was by 2 K smaller per additional CH_2 group in the side chain.

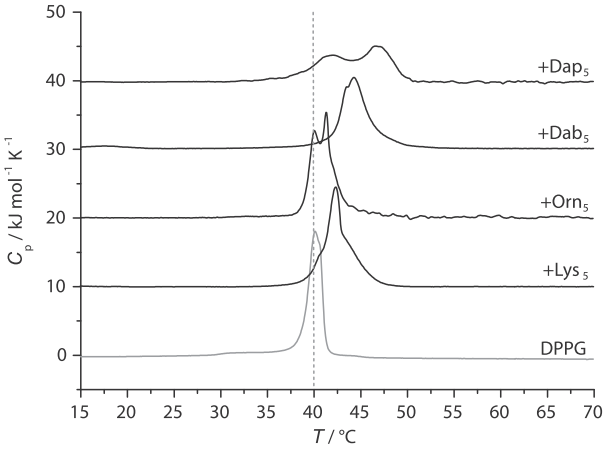

Fig. 4. DSC thermograms of DPPG and DPPG–peptide mixtures ($R_c = 1$). All curves originate from the third heating scan and are shifted vertically for clearness. The dotted line is a guide for the eye indicating T_{m} of pure DPPG vesicles (100 mM NaCl, 1 mM pentapeptide based on monomeric units and 1 mM DPPG, 1 °C min^{-1} heating rate, 4 s time resolution).

Table 2
Phase transition temperatures T_{melt} of DPPG and its mixtures with the peptides at $R_c = 1$, obtained from DSC (global maxima of the heating scans) and from the wavenumber shift of the $\nu_s(CH_2)$ band of DPPG in FT-IR spectra (cooling scans). The shift of the phase transition temperature, ΔT_{melt}, with respect to pure DPPG is also included. Additionally, T_{mid}, obtained from the midpoint of the integral of the curves is given. (DSC: 100 mM NaCl, 1 mM pentapeptide based on monomeric units and 1 mM DPPG, 1 °C min^{-1} heating rate, 4 s time resolution, FT-IR: 100 mM NaCl in D_2O, 60 mM pentapeptide based on monomeric units and 60 mM DPPG, 8 min equilibration time after each temperature step of 2 °C, 32 scans with 2 cm^{-1} spectral resolution).

Sample	T_{mid}/°C	T_{melt}/°C		ΔT_{melt}/°C	
	DSC	DSC	FT-IR	DSC	FT-IR
DPPG	40.0	40.1	41.5		
DPPG/Lys_5	42.4	42.4	42.3	2.1	0.8
DPPG/Orn_5	41.0	40.6	42.0	0.5	0.5
DPPG/Dab_5	44.3	44.3	43.6	4.2	2.1
DPPG/Dap_5	44.4	46.7 (and 41.9)	46.2	6.6	4.7

A suppression of the pre-transition and multi component melting transitions were also found by Carrier et al. [23,46], Schwieger et al. [47] and Papahadjopoulos [19] for DPPG polylysine complexes and by Kleinschmidt et al. for DMPG–pentalysine complexes [31].

The increase in T_{melt} is typically due to electrostatic binding. Due to the shielding of the head group charges after binding the lateral repulsion between the lipids is reduced and therefore the gel phase is stabilized. This was found in many cases where purely electrostatic binding occurs. Papahadjopoulos et al. [19] investigated a range of different membrane binding proteins and found an increase in the lipid main phase transition temperature for mainly electrostatically binding proteins. Likewise, T_{melt} is increased when bound multivalent cations screen head group charges and decrease repulsive electrostatic interactions within the lipid layer [48]. The theoretically predicted increase in the phase transition temperature as a consequence of a complete shielding of all head group charges is 5.5 K [49]. The ΔT_{melt} of 4.7–6.6 K found for Dap_5 (Table 2) can therefore be attributed to mainly electrostatic binding of Dap_5 to DPPG membranes. All peptides in this study are formally equally charged. However, the calculated electrostatic contribution to the free energy of binding and thus on ΔT_{melt} is probably slightly increasing with decreasing side chain length, as the charge density increases. The experimentally observed effect on T_{melt} is different. With increasing length of the side chain the shift in T_{melt} decreases.

Our explanation is that this is most likely due to additional hydrophobic interactions of the longer peptide side chains with the lipids [45]. An insertion of molecules into the fluid membrane driven by hydrophobic interactions typically leads to a decrease in the transition temperature [19]. This can be understood as freezing point depression. In the case of binding of cationic pentapeptides to negatively charged membranes, this freezing point depression counteracts the electrostatic effect, which would lead to an increase in T_{melt}. The hydrophobic contribution depends on the length of the hydrophobic peptide side chains. The longer the side chain is, the more is the electrostatic effect compensated, resulting in a lower increase in T_{melt}. Such a compensation of hydrophobic and electrostatic interactions leading to almost no overall effect on T_{melt} was also observed and discussed before [45]. In our study, ΔT_{melt} in the system DPPG–Orn_5 showed a slight deviation from the expected behavior. However, as seen in Table 2 the values for ΔT_{melt} were more in line with expectations when the FT-IR data were used (described below).

In our DSC experiments we used for all peptides a ratio of $R_c = 1$, i.e. formal charge compensation should occur. The question arose whether the differences observed in T_{melt} are due to different degrees

of binding. For Lys_5 binding to pure DMPG bilayers at 30 °C in the fluid state and in the presence of 100 mM salt the binding constant was determined to ca. 2–2.5 $10^5\ M^{-1}$ (unpublished data, see also Table 1 for binding constants of Dab_5 and Dap_5 and predictions by Ben-Tal et al. [11]). Using this value for the binding constant one can calculate a degree of binding of the peptide of ca. 0.9 under our experimental conditions. A decrease in the binding constant by a factor of two would change the degree of binding by only 2%. As we have mentioned above, shortening of the side chains lead to a higher charge density and thus a higher electrostatic contribution to the free energy of binding. However, this seems to be even over-compensated by a decrease of the hydrophobic contribution, so that the binding constant decreases slightly (see Table 1). We therefore conclude that the degree of binding is very similar for all peptides studied so that the observed differences in T_{melt} are not caused by significantly different degrees of binding.

3.3. FT-IR spectroscopy: effects of peptide binding on lipid organization and hydration

We used FT-IR spectroscopy, a method sensitive to lipid conformational changes, to examine the influence of peptide binding on lipid vesicles in terms of acyl chain organization and hydration of the lipid head groups. Temperature dependent IR measurements can reveal the influence of the peptide binding on the lipid phase behavior.

3.3.1. Acyl chain region of lipids

The influence of peptide binding on the hydrophobic core region of the membranes was monitored using the position of the symmetric CH_2 stretching vibration ($\nu_s(CH_2)$) as indicator (Fig. 5). During the lipid phase transition from gel to fluid phase, the number of *gauche* conformers in the lipid chains increases. The wavenumber of $\nu_s(CH_2)$ then shifts from values typically slightly below 2850 cm^{-1} for gel phase lipids to 2852–2853 cm^{-1} for lipids in the liquid–crystalline phase. The midpoint of this shift can be used to determine the phase transition temperature. The T_{melt} values of the mixtures compared to pure DPPG, are also presented in Table 2 together with values obtained from DSC measurements for comparison (see above). Slight differences can be attributed to a possible hysteresis, as the reported DSC data were obtained from the heating scans, while FT-IR T_{melt} values were taken from the cooling scans.

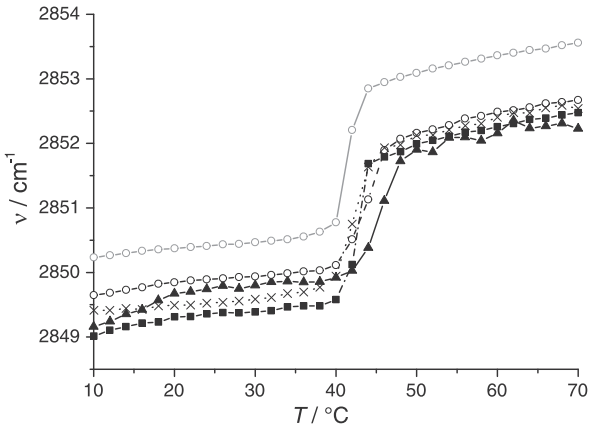

Fig. 5. Wavenumber of the $\nu_s(CH_2)$ vibration observed by FT-IR upon cooling of DPPG containing samples (D_2O, 0.1 M NaCl). DPPG (gray open circles); DPPG/Lys_5 (filled squares); DPPG/Orn_5 (crosses); DPPG/Dab_5 (open circles); DPPG/Dap_5 (filled triangles) (100 mM NaCl in D_2O, 60 mM pentapeptide based on monomeric units and 60 mM DPPG, 8 min equilibration time after each temperature step of 2 °C, 32 scans with 2 cm^{-1} spectral resolution).

Table 3
Shift of the wavenumber of the CH_2 stretching vibration (of $\nu_s(CH_2)$) observed by FT-IR for DPPG/peptide mixtures with respect to pure DPPG in the gel state ($\Delta\nu_s(CH_2)_{30\ °C}$) or fluid state ($\Delta\nu_s(CH_2)_{50\ °C}$) (100 mM NaCl in D_2O, 60 mM pentapeptide based on monomeric units and 60 mM DPPG, 8 min equilibration time after each temperature step of 2 °C, 32 scans with 2 cm^{-1} spectral resolution).

Sample	$\Delta\nu_s(CH_2)_{30\ °C}$ /cm^{-1}	$\Delta\nu_s(CH_2)_{50\ °C}$ /cm^{-1}
DPPG		
DPPG/Lys_5	−1.08	−1.10
DPPG/Orn_5	−0.89	−0.99
DPPG/Dab_5	−0.53	−0.90
DPPG/Dap_5	−0.66	−1.18

A decrease in wavenumber to lower values can be observed at all temperatures, when the various peptides are bound to the lipid (Table 3). This decrease in wavenumber is larger for fluid phase lipids than for gel phase lipids. For gel phase binding, the magnitude of the decrease depends on the length of the side chains of the bound peptide: The effect is the more pronounced, the longer the peptide side chain is. For binding to fluid phase vesicles, the decrease in wavenumber is similar for all interacting peptides.

Such a decrease in the $\nu_s(CH_2)$ wavenumber is typically interpreted as an increased ordering of the lipid acyl chains [50,51]. However, an increased chain order in the gel state should lead to a more marked increase in T_{melt} than we actually determine by DSC or FT-IR. We believe, therefore, that a contribution of an increased vibrational coupling of the CH_2 groups within one chain or between neighboring acyl chains is occurring. Peptide binding to the lipid headgroups might restrict the lipid motion and decrease the rotational freedom of the acyl chains. Such a reduction of the rotational motion is known to decrease the $\nu_s(CH_2)$ wavenumber [52]. As Lys_5 is inserting deeper into the gel phase membrane (see below), it has a higher influence on the rotational mobility of the lipids than Dab_5 (interacting more superficially). This is reflected by the slightly stronger effect on the wavenumber of the $\nu_s(CH_2)$ stretching vibration for Lys_5. Similar shifts were observed before for interaction of divalent cations [42] and the binding of polylysines to lipids [47]. Also, Marsh et al. [53] found that membrane associated proteins increase the packing density and reduce thereby lipid chain motion and Kleinschmidt et al. [31] described lower chain mobility in DMPG–Lys_5 complexes examined by electron paramagnetic resonance correlation techniques.

3.3.2. Headgroup region of lipids

The frequency of the lipid ester carbonyl stretching vibration is indicative for changes in hydration in the lipid head group region. The frequency of this band depends on the number and strength of H-bonds at the C═O group. In D_2O, it is a superposition of bands at 1741 cm^{-1} and 1722 cm^{-1} [54]. The band at higher wavenumbers originates from non-hydrogen-bonded C═O groups, while the one at lower wavenumbers can be assigned to a C═O group having one hydrogen-bond to a water molecule [54–56]. Additional H-bonds lead to additional band components at even lower wavenumbers [54]. The relative changes in hydrogen-bonding can be obtained by fitting Gaussian–Lorentzian functions to the experimental bands [55,57,58].

For pure DPPG vesicles, a clear change in the hydrogen-bonding occurs at the lipid phase transition. The overall band shape changes and fits of Gaussian–Lorentzian functions lead to the finding that DPPG is more hydrated, i.e. the water has more or higher ordered hydrogen-bonds to the C═O groups in the fluid phase than in the gel phase of DPPG [54,55]. Fig. 6A shows the carbonyl vibrations of DPPG–Dab_5 mixtures below (20 °C) and above (60 °C) the lipid phase transition temperature. The general shape of the C═O band is similar for pure DPPG and the other DPPG–peptide mixtures at the

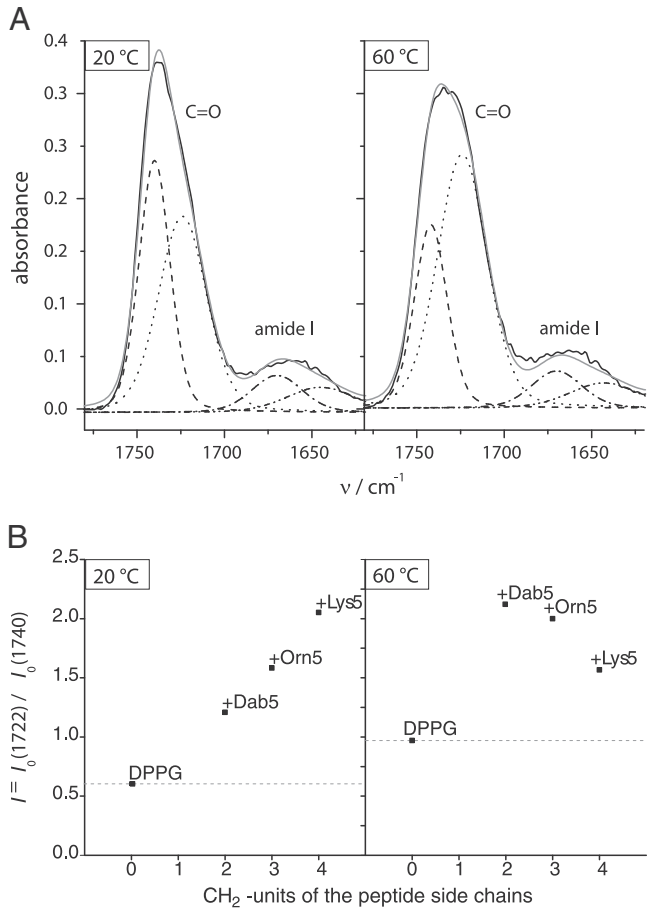

Fig. 6. A: carbonyl and amide I bands observed by FT-IR and fitted band components of a DPPG–Dab_5 mixture at 20 °C (left panel) and 60 °C (right panel). Experimental (solid line), sum fit (gray line) and fitted bands (broken lines). (100 mM NaCl in D_2O, 60 mM Dab_5 based on monomeric units and 60 mM DPPG, 8 min equilibration time after each temperature step of 2 °C, 32 scans with 2 cm^{-1} spectral resolution) B: ratio of integrated intensities of fitted C═O band components $I = I_0(1722\ cm^{-1})/I_0(1740\ cm^{-1})$ as function of peptide side chain length. The band components could not be obtained for DPPG/Dap5 due to superposition of the amide I and C═O band.

respective temperatures (data not shown). In Fig. 6B, the ratio of the integrated intensity of the component for hydrogen-bonded (lower wavenumber) to non-hydrogen-bonded (higher wavenumber) species are depicted for pure DPPG and the different lipid–peptide mixtures. A higher value is due to more or better oriented hydrogen bonds at the lipid C═O group [17]. In the lipid gel phase as well as in the fluid phase, the binding of peptides led to better or more hydrogen-bonding with respect to pure DPPG. The binding of the peptides might facilitate the access of water molecules to the hydrophobic–hydrophilic interface. More likely is that hydration water molecules are shared by the lipid and the bound peptide, [47,59] so that the water molecules become better oriented. This signifies also that the peptide side chains insert into the lipid head group region. At 20 °C, when the lipid vesicles are in the gel phase, binding of the peptides increases the number or improves the orientation of the hydrogen-bonds the longer the side chains are. For binding to the fluid phase, however, the shorter side chain peptides (i.e. the smaller molecules) have a bigger impact on hydrogen-bonds. The different tendencies in the head group hydration of the gel phase and fluid phase are probably due to the different balances of electrostatic and hydrophobic contributions to the peptide binding to the respective phase.

Data for the complex DPPG–Dap_5 are not included in Fig. 6B, because a fit of the carbonyl band was not possible due to an overlap with Dap_5 amide I band of the peptide (see below).

Similar results on changes in hydrogen-bonding have been obtained before in binding studies using poly-L-lysines. Schwieger et al. [47] also found stronger hydrogen-bonds of water to C═O groups in complexes of DPPG with PLL compared to pure DPPG in the gel phase.

3.3.3. Amide bands of peptides

The amide I bands as indicator for the peptide conformation and hydrogen-bonding of the peptide backbone are not changing upon interaction with lipids (data not shown). The peptides are too short to form α-helices or intramolecular β-sheets, but may adopt other rigid conformations. By increasing the pH to values where side chains are uncharged and do not repel each other electrostatically [60], we verified that the peptides are not able to form intermolecular β-sheets (data not shown). Furthermore, no indications for hydrogen bonds between the side chain-NH_3^+-group and the amide group were observed, though they could be expected for Dap_5 having the shortest side chain. Instead, the position of amide I bands shifts to slightly higher wavenumber as the peptide side chain gets shorter, leading to a partial overlap with the lipid carbonyl vibration for the complex DPPG/Dap_5.

All FT-IR experiments were repeated using DMPG–peptide mixtures and yielded qualitatively the same results as discussed for DPPG (data not shown).

3.4. Interaction of pentapeptides with PG monolayers

Lipid monolayers are convenient model systems for studying the binding of molecules to lipids as the change in area or film pressure can be recorded after injection of interacting molecules into the subphase. When peptides are injected underneath a lipid monolayer, two scenarios can be expected: i). Condensation of the monolayer due to electrostatic interactions leading to shielding of the head group charges. Then, a decrease in surface pressure is observed when the total area of the monolayer is constant. ii). Insertion of the peptides into the monolayer due to hydrophobic interactions. Peptides with hydrophobic side chains are able to insert deeper into the lipid layer thereby interacting with the acyl chains. As the peptides are located between the lipid molecules, the surface pressure will increase at constant total area [19]. These two effects counteract when peptides are charged on the one hand, and have hydrophobic side chains on the other hand [45].

To elucidate the balance of the two types of interactions, the adsorption of the model peptides to DPPG monolayers of different initial packing densities, i.e. different initial surface pressure π_0 was investigated. Stock solutions of the pentapeptides were injected underneath DPPG monolayers of defined π_0 at a constant surface area. Pressure changes resulting from the binding of the peptides to the monolayer are shown in Fig. 7B. In most cases, the pressure did not change any more after a waiting period of 10 min. In the case of Dap_5, the equilibration time was somewhat longer. A reason for these slower kinetics of binding might be the fact that in solution Dap_5 has less than five positive charges due to the lower *pK* of 6.33 of the side chains [37] so that the accumulation at the monolayer due to electrostatic attraction to the negatively charged interface is initially lower than for the other peptides. Only after binding to the negatively charged lipids the full charge of +5 develops due to the change in apparent *pK* induced by the negative surface potential (see above). In independent experiments, it was found that the peptides alone are not surface active at this concentration as no change in surface pressure was observed (data not shown).

At low initial surface pressures of the DPPG monolayer ($\pi_0 =$ 12 mN/m), all the peptides induced a decrease in surface pressure, i.e., a condensation of the lipid monolayer. For the peptides with shorter side chains, the condensation is more pronounced. Consequently, injection of Dap_5 resulted in the largest decrease in surface

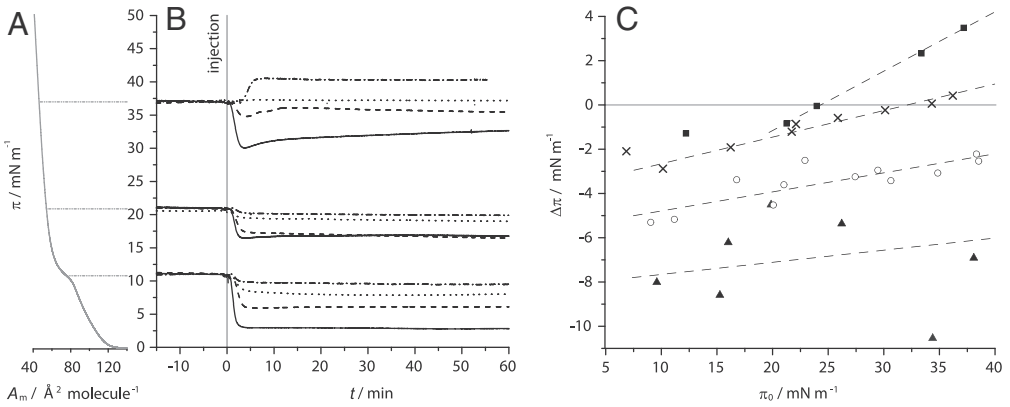

Fig. 7. A: π-*A*-isotherm of a DPPG monolayer; B: surface pressure change during adsorption of different pentapeptides (Lys_5 (dash–dotted); Orn_5 (dotted); Dab_5 (dashed) and Dap_5 (solid)) after injection into the subphase underneath a DPPG layer at constant surface area and at a initial surface pressure of 11 mN m^{-1}, 21 mN m^{-1} and 37 mN m^{-1}; C: absolute pressure changes, $\Delta\pi$, 10 min after injection of the peptide underneath DPPG monolayers, versus the initial surface pressure π_0; Lys_5 (filled squares); Orn_5 (crosses); Dab_5 (open circles); and Dap_5 (filled triangles). To guide the eye, linear regressions are included. (20 °C, 0.1 M NaCl, 15 μM pentapeptides based on monomeric units in bulk, DPPG spread from 0.7 M solution in chloroform/methanol).

pressure. At higher π_0 (21 mN/m), the tendency remains the same, but the decrease in surface pressure becomes smaller. At even higher initial surface pressures ($\pi_0 = 37$ mN/m), the shape of the $\pi - t$ − isotherms for Dap_5 and Dab_5 binding indicate a two-step process. A fast decrease in pressure reflects the condensation of the film and is followed by a slow increase in surface pressure as expected for partial insertion of the peptides. The condensation effect decreases when the peptide side chain is becoming longer from Dap_5 to Lys_5. Injection of Lys_5 and Orn_5 at high π_0 values even leads to an overcompensation of the condensation effect, i.e., to an increase in surface pressure.

The condensation is expected since all peptides are positively charged at the lipid layer and thus compensate the negative DPPG head group charges. This is the same effect that leads to the increase in the transition temperature of bilayers as observed by DSC. That the condensing effect becomes smaller with higher π_0 can also be easily explained, because the initial monolayer is already more condensed, i.e. the available area per molecule is smaller. The fact that the condensing effect becomes smaller with increasing side chain length shows again that another contribution to the binding affinity must be present besides the pure electrostatic interaction. This is the insertion of the peptide side chains into the lipid monolayer driven by hydrophobic effects that then leads to a surface pressure increase. This increase partially compensates the expected decrease due to electrostatic condensation. The propensity for insertion is higher for peptides with longer side chains. Therefore, we observe the largest decrease in surface pressure after injection of Dap_5, which binds mainly electrostatically, and less decrease when the peptide side chain is longer. The increase in surface pressure that follows the insertion of peptide side chains into the lipid monolayer is the more pronounced as the higher the initial surface pressure π_0 is. This is due to a steeper $\pi - A$ isotherm (Fig. 7A), i.e., a lower compressibility, at high π_0. Consequently, reduction of the available area per lipid molecule (A_M) by a certain percentage leads to a larger increase in π. At high π_0, this effect even results in an overcompensation of the condensation, when Lys_5 or Orn_5 are injected (Fig. 7B and C), i.e., to an increase in surface pressure upon insertion.

In Fig. 7C, the absolute pressure changes $\Delta\pi$ 10 min after the injection of the peptide are plotted versus the initial surface pressure π_0. The superposition of the condensing effect that leads to a negative $\Delta\pi$ on the one hand, and the insertion resulting in a positive $\Delta\pi$ can nicely be seen. $\Delta\pi$ becomes more positive i) the higher the initial surface pressure π_0 is and ii) the longer, i.e., the more hydrophobic the peptide side chain is. Similar effects were observed before for binding of poly-L-arginine to negatively charged lipid monolayers. In this case the arginine side chains are even more hydrophobic due to the delocalized charge of the guanidinium moiety at the end of the side chain [45].

The results of the monolayer study supports the finding of reduced rotational freedom of the lipid chains after binding as observed by FT-IR (see above). The deeper insertion of peptides with long side chains hinders lipid rotation more than superficial electrostatic adsorption of peptides with short side chains. In conclusion, the monolayer study shows again the delicate interplay of opposite effects caused by electrostatic as well as hydrophobic contributions occurring in peptide–lipid interactions.

4. Conclusions

Our study focused on the discrimination of electrostatic and hydrophobic contributions to the interaction of short basic peptides with anionic lipid model membranes. The chosen model system consists of DPPG monolayers or vesicles and homopentapeptides composed of lysine (Lys) or analog amino acids with shorter side chains (ornithine (Orn), diaminobutyric acid (Dab) and diaminopropionic acid (Dap)). These model peptides with varying hydrophobic molecular surfaces at constant overall charge enabled the dissection of electrostatic and hydrophobic contributions to the binding. The binding was found to be a process consisting of partially compensating effects. This compensation of counteracting effects was particularly evident in the case of pentalysine interaction where only very small or no overall effects were observed for the binding as studied by ITC. Exothermic and endothermic contributions to the binding enthalpy compensated and, effects on T_m almost leveled out. Pressure changes due to insertion or condensation of a lipid monolayer had equal but opposite values, leading to overall small pressure changes for Lys_5. The shortening of the hydrophobic hydrocarbon spacer of the amino acid side chain in the peptides going from Lys_5 (Orn_5 and Dab_5) to Dap_5 results in a binding mode which is increasingly dominated by electrostatic effects. This was particularly evident for the peptide with the shortest side chain Dap_5.

The ITC data indicated that electrostatic binding was connected with an exothermic heat of reaction, as the peptides with the shorter side chain showed exothermic heats of binding. This exothermic effect is probably caused by a condensation of the lipids, as observed in the monolayer experiments. For Dap_5 particularly high exothermic heats of titration were observed. These are caused by the protonation of the Dap_5 side chains upon binding to the negatively charged lipid surface due to the increase in *pK* of the side chains. In the case of

the pentapeptides with the longer side chains, the intercalation into the head group region due to increase in hydrophobic interactions finally leads to an endothermic heat of binding as observed for Lys_5. Also, the changes in T_{melt} reflect the varying contributions of electrostatic and hydrophobic effects. This increase in T_{melt} is larger for peptides with shorter side chains as expected for more electrostatic interactions, due to reduction of head group–head group repulsion and therefore stabilizing the lipid layer. The largest increase in T_{melt} is attributed to electrostatic interactions and amounts to up to ~5 K for the system Dap_5 and DPPG. The opposing electrostatic and hydrophobic effects could nicely be dissected in monolayer studies. We found that condensation for mainly electrostatically interacting peptides with short side chains (Dab_5 and Dap_5) was counterbalanced by insertion of hydrophobic side chains with increasing side chain length. This tendency resulted in an increase in surface pressure after injection of Lys_5 underneath DPPG at high initial surface pressures π_0.

The findings for Lys_5 presented here are in contrast to results published by Ben-Tal et al. [11] who proposed that no insertion of Lys_5 into the head group region occurs. This was also suggested by various other groups [10–14]. However, summarizing our findings, we believe that we could convincingly show that in the case of Lys_5, compensation effects of hydrophobic and electrostatic contributions to the binding can result in a misleading conclusion when only this particular peptide is investigated. Only the systematic approach presented here using peptides with different side chain lengths is capable of dissecting the two effects and can show the varying contributions as a function of side chain length.

Acknowledgements

We thank K. Brandenburg from in the Leibniz-Center for Medicine and Biosciences, Borstel, Germany for providing the peptides. Financial support by the Deutsche Forschungsgemeinschaft through GRK 1026 “Conformational transitions in macromolecular interactions” is gratefully acknowledged.

References

[1] D. Murray, N. Ben-Tal, B. Honig, S. McLaughlin, Electrostatic interaction of myristoylated proteins with membranes: simple physics, complicated biology, Structure 5 (1997) 985–989.
[2] S. McLaughlin, G. Hangyas-Mihalyne, I. Zaitseva, U. Golebiewska, Reversible-through calmodulin-electrostatic interactions between basic residues on proteins and acidic lipids in the plasma membrane, Biochem. Soc. Symp. 72 (2005) 189–198.
[3] J. Kim, M. Mosior, L.A. Chung, H. Wu, S. McLaughlin, Binding of peptides with basic residues to membranes containing acidic phospholipids, Biophys. J. 60 (1991) 135–148.
[4] J. Kim, P.J. Blackshear, J.D. Johnson, S. McLaughlin, Phosphorylation-reverses the membrane association of peptides that correspond to the basic domains of MARCKS and neuromodulin, Biophys. J. 67 (1994) 227–237.
[5] C.A. Buser, C.T. Sigal, M.D. Resh, S. McLaughlin, Membrane binding of myristylated peptides corresponding to the NH2 terminus of Src, Biochemistry 33 (1994) 13093–13101.
[6] S.E. Blondelle, K. Lohner, M.I. Aguilar, Lipid-induced conformation and lipid-binding properties of cytolytic and antimicrobial peptides: determination and biological specificity, Biochim. Biophys. Acta 1462 (1999) 89–108.
[7] R.M. Epand, H.J. Vogel, Diversity of antimicrobial peptides and their mechanisms of action, Biochim. Biophys. Acta 1462 (1999) 11–28.
[8] K. Matsuzaki, Why and how are peptide–lipid interactions utilized for self-defense? Magainins and tachyplesins as archetypes, Biochim. Biophys. Acta 1462 (1999) 1–10.
[9] N. Sitaram, R. Nagaraj, Interaction of antimicrobial peptides with biological and model membranes: structural and charge requirements for activity, Biochim. Biophys. Acta 1462 (1999) 29–54.
[10] J. Dufourcq, J.F. Faucon, R. Maget-Dana, M.P. Pileni, C. Helene, Peptide–membrane interactions. A fluorescence study of the binding of oligopeptides containing aromatic and basic residues to phospholipid vesicles, Biochim. Biophys. Acta 649 (1981) 67–75.
[11] N. Ben-Tal, B. Honig, R.M. Peitzsch, G. Denisov, S. McLaughlin, Binding of small basic peptides to membranes containing acidic lipids: theoretical models and experimental results, Biophys. J. 71 (1996) 561–575.
[12] N. Ben-Tal, B. Honig, C. Miller, S. McLaughlin, Electrostatic binding of proteins to membranes. Theoretical predictions and experimental results with charybdotoxin and phospholipid vesicles, Biophys. J. 73 (1997) 1717–1727.
[13] D. Murray, A. Arbuzova, G. Hangyas-Mihalyne, A. Gambhir, N. Ben-Tal, B. Honig, S. McLaughlin, Electrostatic properties of membranes containing acidic lipids and adsorbed basic peptides: theory and experiment, Biophys. J. 77 (1999) 3176–3188.
[14] D. Murray, A. Arbuzova, B. Honig, S. McLaughlin, The role of electrostatic and nonpolar interactions in the association of peripheral proteins with membranes, Curr. Top. Membr. 52 (2002) 277–307.
[15] M. Mosior, S. McLaughlin, Peptides that mimic the pseudosubstrate region of protein kinase C bind to acidic lipids in membranes, Biophys. J. 60 (1991) 149–159.
[16] C. Mangavel, R. Maget-Dana, P. Tauc, J.-C. Brochon, D. Sy, J.A. Reynaud, Structural investigations of basic amphipathic model peptides in the presence of lipid vesicles studied by circular dichroism, fluorescence, monolayer and modeling, Biochim. Biophys. Acta 1371 (1998) 265–283.
[17] S. Castano, B. Desbat, M. Laguerre, J. Dufourcq, Structure, orientation and affinity for interfaces and lipids of ideally amphipathic lytic LiKj(i = 2j) peptides, Biochim. Biophys. Acta 1416 (1999) 176–194.
[18] M. Mosior, S. McLaughlin, Binding of basic peptides to acidic lipids in membranes: effects of inserting alanine(s) between the basic residues, Biochemistry 31 (1992) 1767–1773.
[19] D. Papahadjopoulos, M. Moscarello, E.H. Eylar, T. Isac, Effects of proteins on thermotropic phase transitions of phospholipid membranes, Biochim. Biophys. Acta 401 (1975) 317–335.
[20] H. Takahashi, S. Matuoka, S. Kato, K. Ohki, I. Hatta, Effects of poly(L-lysine) on the structural and thermotropic properties of dipalmitoylphosphatidylglycerol bilayers, Biochim. Biophys. Acta 1110 (1992) 29–36.
[21] W. Hartmann, H.J. Galla, Binding of polylysine to charged bilayer membranes. Molecular organization of a lipid.peptide complex, Biochim. Biophys. Acta 509 (1978) 474–490.
[22] H. Takahashi, T. Yasue, K. Ohki, I. Hatta, Structure and phase behavior of dimyristoylphosphatidic acid/poly(L-lysine) systems, Mol. Membr. Biol. 13 (1996) 233–240.
[23] D. Carrier, M. Pezolet, Investigation of polylysine–dipalmitoylphosphatidylglycerol interactions in model membranes, Biochemistry 25 (1986) 4167–4174.
[24] G. Foerster, C. Schwieger, F. Faber, T. Weber, A. Blume, Influence of poly(L-lysine) on the structure of dipalmitoylphosphatidylglycerol/water dispersions studied by X-ray scattering, Eur. Biophys. J. 36 (2007) 425–435.
[25] A. Arbuzova, L. Wang, J. Wang, G. Hangyas-Mihalyne, D. Murray, B. Honig, S. McLaughlin, Membrane binding of peptides containing both basic and aromatic residues. Experimental studies with peptides corresponding to the scaffolding region of caveolin and the effector region of MARCKS, Biochemistry 39 (2000) 10330–10339.
[26] L.M.S. Loura, A. Coutinho, A. Silva, A. Fedorov, M. Prieto, Structural effects of a basic peptide on the organization of dipalmitoylphosphatidylcholine/dipalmitoylphosphatidylserine membranes: a fluorescent resonance energy transfer study, J. Phys. Chem. B 110 (2006) 8130–8141.
[27] D.J. Mitchell, D.T. Kim, L. Steinman, C.G. Fathman, J.B. Rothbard, Polyarginine enters cells more efficiently than other polycationic homopolymers, J. Pept. Res. 56 (2000) 318–325.
[28] M. Roux, J.M. Neumann, M. Bloom, P.F. Devaux, Deuterium and phosphorus-31 NMR study of pentalysine interaction with headgroup deuterated phosphatidylcholine and phosphatidylserine, Eur. Biophys. J. 16 (1988) 267–273.
[29] B. Bonev, A. Watts, M. Bokvist, G. Grobner, Electrostatic peptide-lipid interactions of amyloid-b peptide and pentalysine with membrane surfaces monitored by 31P MAS NMR, Phys. Chem. Chem. Phys. 3 (2001) 2904–2910.
[30] N. Ben-Tal, B. Honig, C.K. Bagdassarian, A. Ben-Shaul, Association entropy in adsorption processes, Biophys. J. 79 (2000) 1180–1187.
[31] J.H. Kleinschmidt, D. Marsh, Spin-label electron spin resonance studies on the interactions of lysine peptides with phospholipid membranes, Biophys. J. 73 (1997) 2546–2555.
[32] G. Denisov, S. Wanaski, P. Luan, M. Glaser, S. McLaughlin, Binding of basic peptides to membranes produces lateral domains enriched in the acidic lipids phosphatidylserine and phosphatidylinositol 4,5-bisphosphate: an electrostatic model and experimental results, Biophys. J. 74 (1998) 731–744.
[33] A.I.P.M. De Kroon, M.W. Soekarjo, J. De Gier, B. De Kruijff, The role of charge and hydrophobicity in peptide–lipid interaction: a comparative study based on tryptophan fluorescence measurements combined with the use of aqueous and hydrophobic quenchers, Biochemistry 29 (1990) 8229–8240.
[34] V.V. Andrushchenko, H.J. Vogel, E.J. Prenner, Optimization of the hydrochloric acid concentration used for trifluoroacetate removal from synthetic peptides, J. Pept. Sci. 13 (2007) 37–43.
[35] I. Avanti Polar Lipids, Determination of Total Phosphorusin, \url, www.avantilipids.com/TechnicalInformation.html, 2008.
[36] M. Schiewek, M. Krumova, G. Hempel, A. Blume, Pressure jump relaxation setup with IR detection and millisecond time resolution, Rev. Sci. Instrum. 78 (2007) 045101/045101-045101/045106.
[37] Y. Lan, B. Langlet-Bertin, V. Abbate, L.S. Vermeer, X. Kong, K.E. Sullivan, C. Leborgne, D. Scherman, R.C. Hider, A.F. Drake, S.S. Bansal, A. Kichler, A.J. Mason, Incorporation of 2,3-Diaminopropionic acid into linear cationic amphipathic peptides produces pH-sensitive vectors, ChemBioChem 11 (2010) 1266–1272.
[38] J.-F. Tocanne, J. Teissié, Ionization of phospholipids and phospholipid-supported interfacial lateral diffusion of protons in membrane model systems, Biochim. Biophys. Acta 1031 (1990) 111–142.

[39] T. Träuble, M. Teubner, P. Wooley, H.J. Eibl, Electrostatic interactions at charged lipid membranes. I. Effects of pH and univalent cations on membrane structure, Biophys. Chem. 4 (1976) 319–342.
[40] R. Lehrmann, J. Seelig, Adsorption of Ca^{2+} and La^{3+} to bilayer membranes: measurement of the adsorption enthalpy and binding constant with titration calorimetry, Biochim. Biophys. Acta 1189 (1994) 89–95.
[41] J. Seelig, Titration calorimetry of lipid–peptide interactions, Biochim. Biophys. Acta 1331 (1997) 103–116.
[42] P. Garidel, A. Blume, Interaction of alkaline earth cations with the negatively charged phospholipid 1,2-Dimyristoyl-*sn*-glycero-3-phosphoglycerol: a differential scanning and isothermal titration calorimetric study, Langmuir 15 (1999) 5526–5534.
[43] G. Montich, S. Scarlata, S. McLaughlin, R. Lehrmann, J. Seelig, Thermodynamic characterization of the association of small basic peptides with membranes containing acidic lipids, Biochim. Biophys. Acta 1146 (1993) 17–24.
[44] S. May, D. Harries, A. Ben-Shaul, Lipid demixing and protein–protein interactions in the adsorption of charged proteins on mixed membranes, Biophys. J. 79 (2000) 1747–1760.
[45] C. Schwieger, A. Blume, Interaction of Poly(L-arginine) with negatively charged DPPG membranes: calorimetric and monolayer studies, Biomacromolecules 10 (2009) 2152–2161.
[46] D. Carrier, J. Dufourcq, J.F. Faucon, M. Pezolet, A fluorescence investigation of the effects of polylysine on dipalmitoylphosphatidylglycerol bilayers, Biochim. Biophys. Acta 820 (1985) 131–139.
[47] C. Schwieger, A. Blume, Interaction of poly(L-lysines) with negatively charged membranes: an FT-IR and DSC study, Eur. Biophys. J. 36 (2007) 437–450.
[48] A. Blume, P. Garidel, in: R.B. Kemp (Ed.), Handbook of Thermal Analysis and Calorimetry, vol. 4, Elsevier, Amsterdam, 1999, pp. 109–173.
[49] G. Cevc, A. Watts, D. Marsh, Non-electrostatic contribution to the titration of the ordered-fluid phase transition of phosphatidylglycerol bilayers, FEBS Lett. 120 (1980) 267–270.
[50] L.K. Tamm, S.A. Tatulian, Infrared spectroscopy of proteins and peptides in lipid bilayers, Q. Rev. Biophys. 30 (1997) 365–429.
[51] D.G. Cameron, H.L. Casal, H.H. Mantsch, Y. Boulanger, I.C.P. Smith, The thermotropic behavior of dipalmitoyl phosphatidylcholine bilayers. A Fourier transform infrared study of specifically labeled lipids, Biophys. J. 35 (1981) 1–16.
[52] V.R. Kodati, R. El-Jastimi, M. Lafleur, Contribution of the intermolecular coupling and librotorsional mobility in the methylene stretching modes in the infrared spectra of acyl chains, J. Phys. Chem. 98 (1994) 12191–12197.
[53] D. Marsh, Lipid–protein interactions in membranes, FEBS Lett. 268 (1990) 371–375.
[54] A. Blume, W. Huebner, G. Messner, Fourier transform infrared spectroscopy of $^{13}C=O$ labeled phospholipids hydrogen bonding to carbonyl groups, Biochemistry 27 (1988) 8239–8249.
[55] W. Hubner, A. Blume, Interactions at the lipid–water interface, Chem. Phys. Lipids 96 (1998) 99–123.
[56] K.B. Patel, G. Eaton, M.C.R. Symons, Solvation spectra. Part 78. Solvation of esters and dialkyl carbonates, J. Chem. Soc., Faraday Trans. 1F 81 (1985) 2775–2786.
[57] A. Meister, A. Blume, Solubilization of DMPC-d54 and DMPG-d54 vesicles with octylglucoside and sodium dodecyl sulfate studied by FT-IR spectroscopy, Phys. Chem. Chem. Phys. 6 (2004) 1551–1556.
[58] E. Muller, A. Giehl, G. Schwarzmann, K. Sandhoff, A. Blume, Oriented 1,2-dimyristoyl-*sn*-glycero-3-phosphorylcholine/ganglioside membranes: a Fourier transform infrared attenuated total reflection spectroscopic study. Band assignments; orientational, hydrational, and phase behavior; and effects of Ca^{2+} binding, Biophys. J. 71 (1996) 1400–1421.
[59] R.N.A.H. Lewis, R.N. McElhaney, W. Pohle, H.H. Mantsch, Components of the carbonyl stretching band in the infrared spectra of hydrated 1,2-diacylglycerolipid bilayers: a reevaluation, Biophys. J. 67 (1994) 2367–2375.
[60] M. Jackson, P.I. Haris, D. Chapman, Conformational transitions in poly(L-lysine): studies using Fourier transform infrared spectroscopy, Biochim. Biophys. Acta 998 (1989) 75–79.